Performance Analysis of a Utility-Scale Wave Energy Converter

by
Nicholas May-Varas

A THESIS

submitted to

Oregon State University

Honors College

in partial fulfillment of
the requirements for the
degree of

Honors Baccalaureate of Science in Mechanical Engineering
(Honors Scholar)

Presented December 6, 2021
Commencement June 2022

AN ABSTRACT OF THE THESIS OF

Nicholas May-Varas for the degree of Honors Baccalaureate of Science in Mechanical Engineering presented on December 6, 2021. Title: Performance Analysis of a Utility-Scale Wave Energy Converter.

Abstract approved: _____

Bryson Robertson

A six degree of freedom (6DOF) point-absorber wave energy converter (WEC) called LUPA is being developed at Oregon State University. This research focused on analyzing a full-scale LUPA, called LUPA20, to answer the following questions: 1) How does a full-scale WEC perform due to various factors; 2) What are the implications of using a mooring system attached to a WEC; 3) How does a mooring system affect the "optimal" power take-off (PTO) damping coefficient; 4) How does a WEC affect the incoming waves? One of the first parts of this research consisted of conducting an exhaustive power take-off (PTO) damping coefficient search to obtain the "optimal" PTO damping coefficients of LUPA20. Those "optimal" PTO damping coefficients were used to determine the energy production of LUPA20. The results indicate that LUPA20 has an approximate power rating of 96 KW when analyzing the average power results of time domain simulations using a certain range of sea states. To develop a comprehensive LUPA20 model, a mid-water float mooring setup was implemented into the LUPA20 time domain simulations. Simulations were run using various extreme sea states to determine the effects mooring lines might have on LUPA20. The power results indicate the mooring lines have a relatively large effect on the power production. This is evident in the 4.7% difference between the peak power values and the 6.9% difference between the average power values. A PTO damping coefficient sensitivity study was conducted to determine whether the "optimal" PTO damping coefficient change when mooring lines are implemented. The PTO damping coefficient sensitivity study indicated mooring lines do not have a significant effect on the "optimal" PTO damping coefficient. As well as understanding the effects mooring lines have on WEC performance, understanding the effects LUPA20 has on the incoming waves was also studied. A transmission coefficient (K_t) analysis was conducted to determine how much energy LUPA20 is absorbing from the incoming waves.

The minimum K_t is 0.84, which indicates LUPA20 can absorb a maximum of approximately 16% of the incoming wave energy.

Key Words: Wave energy, numerical modeling, utility-scale

Corresponding e-mail address: bryson.robertson@oregonstate.edu

Performance Analysis of a Utility-Scale Wave Energy Converter

by
Nicholas May-Varas

A THESIS

submitted to

Oregon State University

Honors College

in partial fulfillment of
the requirements for the
degree of

Honors Baccalaureate of Science in Mechanical Engineering
(Honors Scholar)

Presented December 6, 2021
Commencement June 2022

Honors Baccalaureate of Science in Mechanical Engineering project of Nicholas May-Varas presented on December 6, 2021.

APPROVED:

_____

Bryson Robertson, Mentor, representing Civil and Construction Engineering

_____

Solomon Yim, Committee Member, representing Civil and Construction Engineering

_____

Pedro Lomónaco, Committee Member, representing Civil and Construction Engineering

_____

Bret Bosma, Committee Member, representing Civil and Construction Engineering

_____

Toni Doolen, Dean, Oregon State University Honors College

I understand that my project will become part of the permanent collection of Oregon State University, Honors College. My signature below authorizes release of my project to any reader upon request.

_____

Nicholas May-Varas, Author

Table of Contents

Introduction

Wave energy converters (WECs) are devices that extract energy from waves and according to the U.S. Energy Information Administration, there is about 2.64 trillion kilowatt-hours of energy potential in waves of the coasts of the United States [1]. Using more renewable energy technologies, such as WECs, is critical to ensure a sustainable future. Many contributions have been made to progress the WEC industry by developing innovative WECs and researching the fundamental aspects of WEC dynamics. One of the main goals of WEC development is improving the amount of power that can be generated from incoming waves. This requires understanding the many parameters involved in WEC development, such as the power take-off (PTO) damping coefficient and the mooring setup.

One WEC archetype that has continued to be of interest to researchers and technology developers is the point-absorber WEC. A point absorber WEC is a device that generally consists of one or two bodies that are much smaller than one wavelength [2]. The relative movement between a fixed point or between multiple moving bodies produces power [3]. Two examples of point-absorber WECs are shown in Figures 1 and 2.

Figure 1: Ocean Power Technologies' PB3 PowerBuoy® WEC [4]

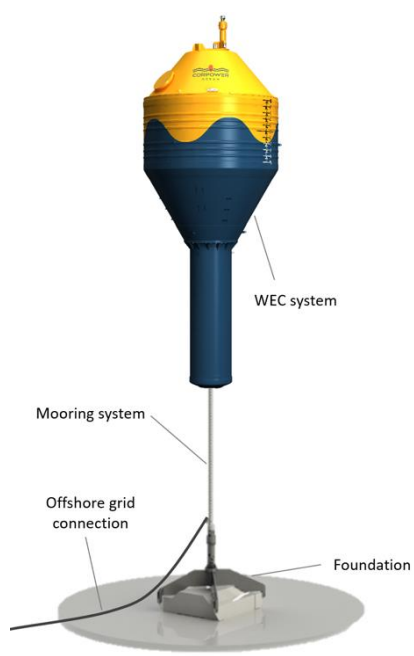

Figure 2: CorPower's Point Absorber WEC [5]

WEC Numerical Modeling

Many numerical setups have been developed for analyzing WECs, which range from using linear systems and nonlinear systems, to using various ways to calculate the forces on a WEC. Zhang et al. [3] studied the effects of implementing a nonlinear setup to analyze a point absorber WEC. They applied a weak-scatter approximation for the simulations and the numerical results showed a difference in the performance between the linear model and the non-linear model for large wave steepness values. Furthermore, the circulated truncated cone buoy tended to have the largest long-term capture power and long-term energy capture width ratio. Vicente et al. [23] compared linear and nonlinear PTO systems. It was determined that the nonlinear PTO system, which was a hydraulic PTO system, affected the horizontal motion and absorbed power of the WEC. Also, the frequency domain surge motion amplitude results and the time domain surge motion amplitude results for the linear PTO system had differences between each other. Another study comparing linear and nonlinear PTO systems was conducted by Zhang et al. [24]. They studied a linear and nonlinear PTO system, which were a part of a point absorber WEC. The size, shape, and PTO damping coefficient of the WEC were varied to gain a better understanding of the effects that each PTO system had on the WEC's performance. The results showed that the nonlinear point absorber WEC tended to produce more power than the linear point absorber WEC. Heo et al. [25] conducted a numerical study to understand the effects of using two different dynamic analysis methods when analyzing a heaving-point absorber WEC. One method was based on Newton's second law and the other was based on the multibody dynamics' formulation. The analysis of the Response Amplitude Operator showed similar results for both methods. A linear analysis of used in this research, which provides a baseline methodology to better understand the performance of the WEC studied in this research and future work could incorporate nonlinear analyses.

WEC Experimental and Numerical Research

To further understand and provide validity to numerical results, comparison studies between numerical and experimental results of point absorbers have been conducted. Beatty et al. [13] conducted an analysis of two point absorber WECs with different reacting bodies and compared Boundary Element Method (BEM) data to experimental data. After comparing the results and incorporating some experimentally derived coefficients into the numerical models,

simulations were run to compare the two WECs. The results indicated that the WEC with a bulbous reacting body had a higher natural frequency than the WEC with a flat plate reacting body, demonstrating the importance to optimize the reacting body geometry based on the most frequent sea state of the WEC deployment site. A comparison study was conducted by Dong et al. [14], which consisted of analyzing various parameters such as heave motion of a WEC's float and the PTO force. After the numerical model was validated, a sensitivity study was conducted with the numerical model. The study led to the conclusion that the wave period can greatly affect the power production of the WEC and there was a linear relationship between the wave heights and the system behavior. Comparison between numerical and experimental results was shown to be critical in research conducted by Rahmati et al. [15]. They analyzed a point absorber called a Wave-driven, Resonant, Arcuate action, Surging point absorber (WRASPA), which was developed by Lancaster University. A main finding from the work is the experimentally determined capture width ratio was between 33% and 60%, while the numerically determined capture width ratio ranged from 140% to 210%. These results were mainly attributed to the viscous effects, separation, and flow rotation not being included in the WAMIT (a wave interaction software capable of obtaining various hydrodynamic coefficients) [16] calculations. The results demonstrate the importance to include those effects in frequency and time domain numerical models. Ma et al. [17] conducted a comparison study of a point absorber, which showed similar results between the experimental and numerical models. Results of a PTO stiffness coefficient analysis indicated that the PTO stiffness coefficient does not affect the power production as much as the PTO damping coefficient. The Wavestar point absorber was analyzed by Ransley et al. [18] to compare a nonlinear coupled Wavestar point absorber model with experimental results. They found the numerical and experimental results were similar for the fixed structure, however the freely pitching cases showed differences in the pressure distribution and the motion of the WEC.

WEC Performance

Power production and overall performance analyses of point absorbers have continued to be a major component of the WEC industry. A study conducted by Arzaghi et al. [6] developed a methodology to predict WEC power production using a Markov Chain model. Three locations were analyzed in the Markov Chain model, which predicted the absorbed power from waves at each location. The results indicated the methodology could provide a reasonable estimation of the

absorbed power from waves at various locations. Another way of understanding the power capabilities of WECs is by analyzing the transmission coefficient. An analysis conducted by Zhao et al. [7] studied parameters such as transmission, reflection, and dissipation coefficients between two breakwater-type WECs. Results indicated that the PTO force does not affect the transmission coefficients as much as the wave number, which shows an important correlation between where the WEC is deployed and the impacts the WEC has on the waves. Piscopo et al. [8] developed a new point absorber design that incorporated a survival mode. The survival mode is useful to prevent significant loading on the WEC during extreme sea states, such as a 50-year storm. The results concluded that their WEC was able to better match the wave climate at each site compared to a reference WEC due to the tuning of added mass, which helped modify the resonance frequency of the WEC.

As well as analyzing the performance of specific point absorber designs, geometric optimization is an important aspect of WEC development. A geometric optimization process conducted by Shadman et al. [9] focused on identifying the optimal draft and buoy diameter of a cylindrical buoy point absorber. They were interested in maximizing the absorbed power of the device and determining a device that had a natural period similar to the predominant wave periods in a nearshore region of the Rio de Janeiro coast. After implementing a design of experiments and analyzing the absorbed power, the optimal draft and buoy diameter were determined to be 3 m. and 13.5 m., respectively. The optimization of a point absorber WEC was also conducted by Piscopa et al. [10] in a study focused on optimizing the PTO damping coefficient and added mass for various size point absorbers. The optimal configuration was determined based on the Annualized Energy Production per unit area and the Levelized Cost of Energy. Their results indicated nondimensional absorbed power and nondimensional energy distributions remained relatively constant throughout a range of tested buoy diameters. Erselcan et al. [11] conducted an optimization study of a point absorber by varying float geometries and PTO parameters. The main goal of the optimization process was to maximize annual energy production. The results indicated the semi-ellipsoid and semi-elliptic floats had similar performance results and the cylindrical floats had poorer performance results. As well as the geometry of point absorbers, the PTO system has been a key research topic. Li et al. [12] analyzed the performance of a PTO system with a mechanical motion rectifier (MMR) and one without an MMR. They determined that both systems perform similarly in large wave periods. Furthermore, a closed form solution of the optimal PTO

damping coefficient for non-MMR was derived, which can reduce computation time when conducting an optimal PTO damping coefficient exhaustive search.

Mooring Analyses

The mooring lines attached to a WEC are another aspect of WEC development that has continued to be studied. Ortiz [19] conducted a mooring optimization analysis for a point absorber WEC. The optimization analysis consisted of varying parameters, such as float diameter, chain diameter, and the number of mooring lines. The optimal mooring configuration total power was approximately 15% more compared to the non-moored cases, when including all the forces acting on the WEC in the power calculation. Cerveira et al. [20] conducted a numerical study of a WEC with three different cases, which consisted of one that did not include mooring, one that had weakly slack mooring, and one with moderately slack mooring. Results indicated that the mooring decreased the annual captured energy by about 1%, when comparing the annual captured energy from the PTO system. Experimental results regarding the effects of moorings on WEC performance have been conducted. Zanuttigh et al. [21] experimentally tested two mooring setups and analyzed the effects of each of them. A spread mooring setup and a catenary anchor leg mooring (CALM) setup were connected to a WEC. The results indicated the CALM mooring system led to larger power production than the spread mooring system, indicating a correlation between mooring line setup and WEC performance. A study conducted by Xu et al. [22] analyzed the effects of various mooring designs attached to a point absorber WEC. The HNBW design, which incorporated clumped weights on the lower part of the mooring system, had a larger peak normalized energy conversion efficiency than the mooring designs without clumped weights.

As evident throughout the literature, the comprehensive analysis of point absorbers is a critical aspect of WEC research. For example, understanding the implications of various simulation setups, which can range from setups being linear or nonlinear models, to the effects of mooring lines and WEC geometries, are critical to understand when researching WECs.

Numerical Modeling Methods

Due to the importance of continuing to study various WEC designs and conducting various parameter studies, the following sections detail the numerical analysis of a point absorber WEC called LUPA being developed at Oregon State University. This study furthers the current work

being conducted by scaling the size of LUPA by 20 times. The 20 times scaled LUPA, which will be referred to as LUPA20, is a point absorber WEC consisting of a spar and a float. The dimensions of the float, spar, and overall device are shown in Figures 3 through 5.

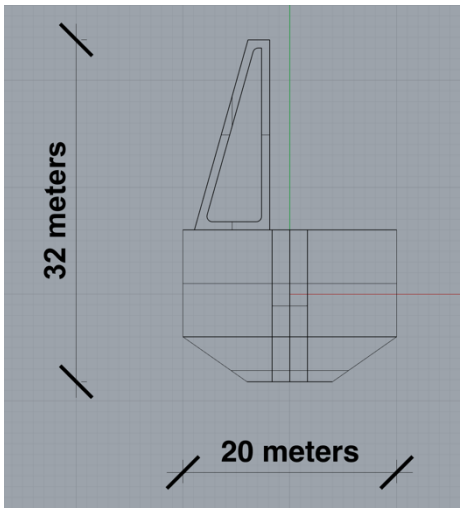

Figure 3: LUPA20 Float

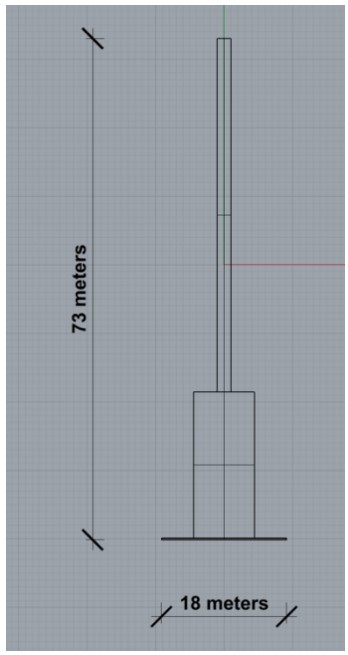

Figure 4: LUPA20 Spar

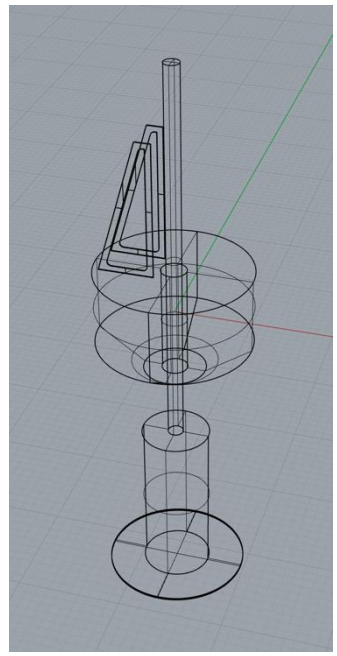

Figure 5: LUPA20

The research focused on the following main questions: 1) How does a full-scale WEC perform due to various wave conditions; 2) What are the implications of using a mooring system attached to a WEC; 3) How does a mooring system affect the "optimal" PTO damping coefficient; 4) How does a WEC affect the incoming waves? Pertaining to the first question, it is critical to continue studying the various factors that affect WEC performance. Power production was a primary parameter analyzed in this research. An exhaustive PTO damping coefficient search and the mean annual energy production analysis are described in the following sections. They are used as a foundation for understanding the power production capabilities of LUPA20. The effects of including mooring lines in numerical simulations will then be discussed by analyzing peak power, average power, and peak-to-average power values between a moored and a free floating design. Regarding the third question, there seems to be a lack of research regarding the effects that a mooring system has on a WEC's "optimal" PTO damping coefficient. Therefore, a PTO damping

coefficient sensitivity analysis was conducted for a setup that includes a mooring design. Another topic that will be discussed is the impact that LUPA20 has on the wave height of the incoming waves. This analysis provides important information regarding the transmission coefficient of LUPA20 in various sea states, which provides a foundation for research to be conducted regarding the performance of an array of LUPA20 devices.

Numerical Modeling

The first step in developing a comprehensive model of LUPA20 entailed meshing and scaling the LUPA20 float and spar in Rhinoceros 3D (Rhino) [26]. Rhino was used to scale the spar and the float geometries by 20 times and then a meshing process was conducted. This process consisted of iteratively meshing the spar and the float by refining the mesh to obtain more accurate Boundary Element Method (BEM) data. BEM data were obtained using WAMIT [16]. WAMIT is a wave interaction software that was used to obtain various hydrodynamic coefficients, such as added mass and radiation damping. The refined meshes of the float and the spar are shown in Figures 6 and 7, respectively.

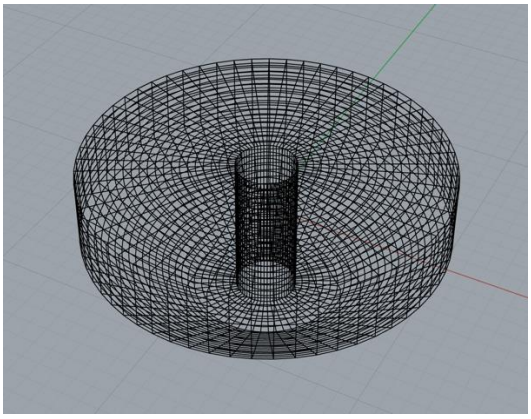

Figure 6: LUPA20 Float Mesh

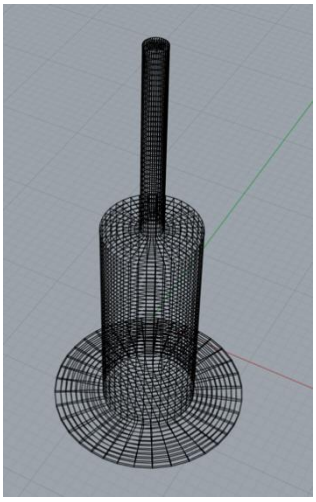

Figure 7: LUPA20 Spar Mesh

WEC-Sim Model

After analyzing the WAMIT results in BEMIO [27], the data were incorporated into the WEC-Sim (a WEC simulation code) [28] setup. Figure 8 shows LUPA20 in WEC-Sim. Drag

coefficients were included into the WEC-Sim setup to improve the accuracy of the results. The float drag coefficient in the z-direction is 1.77 and is based on research conducted by Gu et al. [30]. The drag coefficients for the float, in the x and y-directions, are both 1 and are based on the geometry of the float. The spar drag coefficient in the z-direction is 3.5 and is based on research conducted by Beatty [29]. The drag coefficients for the spar, in the x and y-directions, are both 1 and are based on the geometry of the spar.

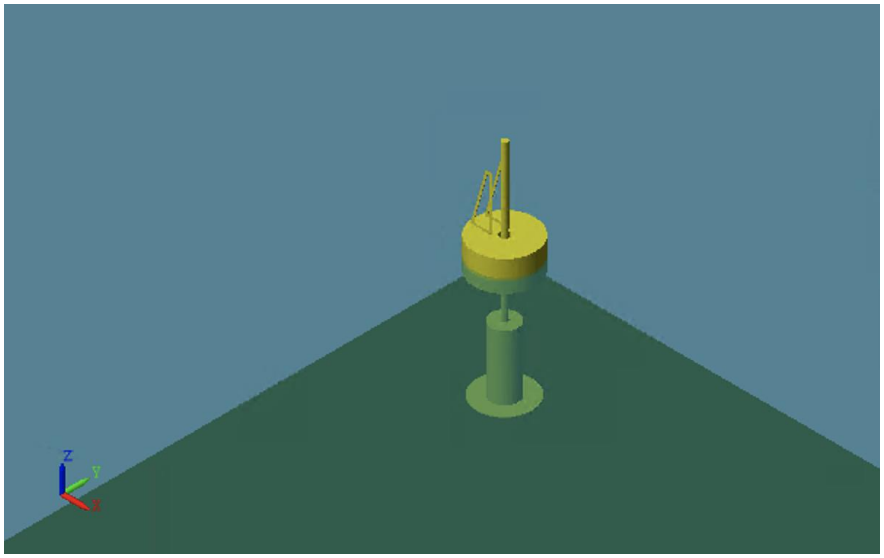

Figure 8: LUPA20 in WEC-Sim

The main equation used to analyze forces on floating bodies is the governing equation of motion based on dynamic equilibrium, which is shown in Eq. 1.

$$m * \ddot{X} = F_{exc} + F_{rad} + F_{pto} + F_{v_{drag}} + F_{hs} + F_{moor} \tag{1}$$

The m and $\ddot{X}$ are the mass of the WEC and the acceleration of the WEC, respectively. F_{exc} and F_{rad} are the excitation force and radiation force, respectively. The excitation force in WEC-Sim is calculated by summing the Froude-Krylov force, which occurs due to the incident waves, and the diffraction loading, which is from the presence of the WEC [28]. F_{rad} is the sum of the added mass and wave damping/radiation forces. F_{pto} is the force on the floating body due to the PTO. F_{pto} is of particular importance in this study due to it being one of the components used to

calculate the average power absorbed by the PTO. Eq. 2 is the equation for the PTO power in terms of the PTO force, F_{pto}, and the relative velocity, v_{rel}, between the spar and the float.

$$P_{pto} = F_{pto} * v_{rel} \tag{2}$$

$F_{v,drag}$ is the drag force, which is based on the drag coefficient, characteristic area, density of the fluid, and the relative velocity between the WEC and the fluid [34]. F_{hs} is the hydrostatic restoring force, which is calculated based on the linear hydrostatic restoring stiffness coefficients obtained from WAMIT [35]. F_{moor} is the mooring force on the floating body and similarly to the hydrostatic restoring force, the mooring force acts as a restoring force on the floating body. There are various ways of modeling mooring lines. For example, in WEC-Sim, the mooring force can be calculated using a linear quasi-static mooring stiffness or there is an option to use a lumped-mass mooring dynamics model [36]. ProteusDS (a marine analysis software) uses a cubic-spline lumped mass cable model, which is able to model torsional and bending parameters [33].

WEC-Sim Power Performance Assessment

After the WEC-Sim setup had been developed, an exhaustive PTO damping coefficient search was conducted using WEC-Sim. The "optimal" PTO damping coefficients were determined based on the corresponding average power produced for each wave period analyzed in the study. Next, the "optimal" PTO damping coefficients were used to analyze the mean annual energy production (MAEP) and individual energy production values of LUPA20. The WEC-Sim simulations were run using wave conditions at PacWave [37], which is a wave energy testing site being constructed off the Oregon Coast. The sea states analyzed in the MAEP analysis were from the PacWave Wave Resource Assessment written by Dunkle et al. [31]. The wave periods ranged from 5 to 12 seconds, the wave heights ranged from 0.5 to 7.5 meters, and the PTO damping coefficients ranged from 4E5 to 5E6 N*s/m. WEC-Sim time-domain simulations were run with irregular waves and for approximately one hour to help ensure the entire wave spectrum was captured. Peak period and significant wave height were used when running irregular waves and the assumption of linear superposition was considered for the analyses. The peak period is the wave period with the highest spectral density in the wave spectrum [32]. As defined in the WEC-Sim manual, significant wave height is "the mean wave height of the tallest third of the waves"

[28]. The significant wave height equation is shown in Eq. 3. The m_0 in Eq. 3 is described in the WEC-Sim manual as the variance of the free surface [28].

$$H_{m0} = 4 * \sqrt{m_0} \tag{3}$$

Following the simulations, the MAEP and individual energy production values were obtained for LUPA20. The MAEP was calculated based on Eq. 4. $\overline{P_{i,j}}$ is the average power for each peak wave period and significant wave height combination analyzed in the MAEP analyses. Each hourly occurrence, denoted by f, that was used in the MAEP calculation was obtained from the PacWave Wave Resource Assessment written by Dunkle et al. [31]. Sea-state data used in this research is from the PacWave Wave Resource Assessment written by Dunkle et al. [31]. The sea-state histogram in the PacWave Wave Resource Assessment written by Dunkle et al. [31] is referred to throughout this research and is shown in Figure 9 [31].

$$MAEP = \sum \overline{P_{i,j}} * f \tag{4}$$

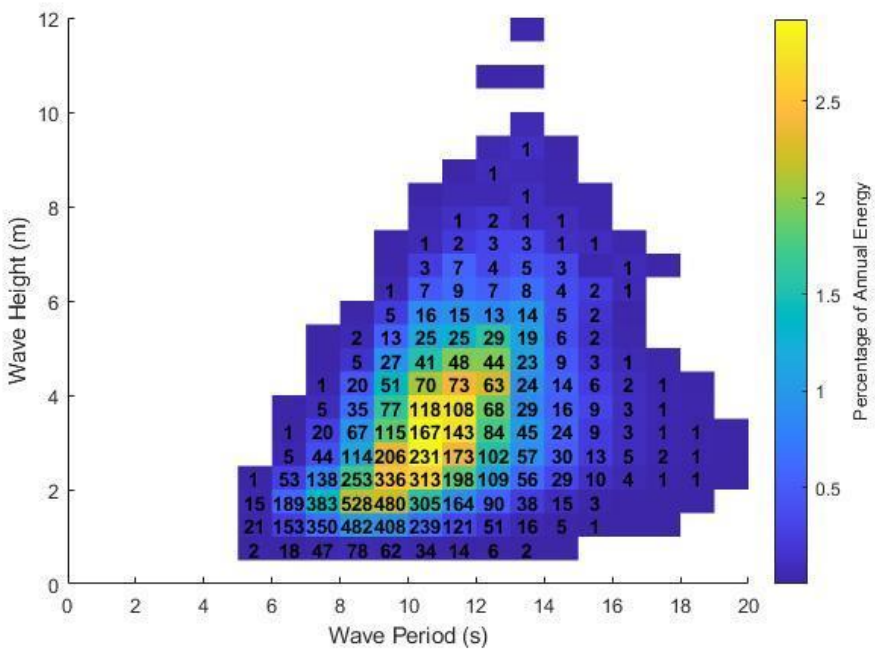

Figure 9: Sea-state histogram in the PacWave Wave Resource Assessment written by Dunkle et al. [31], containing data regarding PacWave South [31].

ProteusDS Model

The power performance of LUPA20 is critical to understand when developing a WEC. However, due to the ocean being very dynamic, WECs will tend to float away from the desired location if a mooring system is not incorporated into them. This is evident in Figure 10, which details the spar position in surge for a mooring and no mooring case. The mooring lines are providing a mean resistant force to LUPA20, which is reducing the distance the LUPA20 is moving. This reduction in the distance LUPA20 moves allows for one to know where LUPA20 will generally be located. However, it is important to understand the effects the mooring system has on the performance of LUPA20 before experimental tests are conducted. This led to a mooring analysis to be conducted in ProteusDS [33]. ProteusDS is a marine analysis software capable of modeling the complex interactions of marine systems and the ocean environment [33]. ProteusDS was used instead of WEC-Sim due to it being able to more accurately model mooring dynamics.

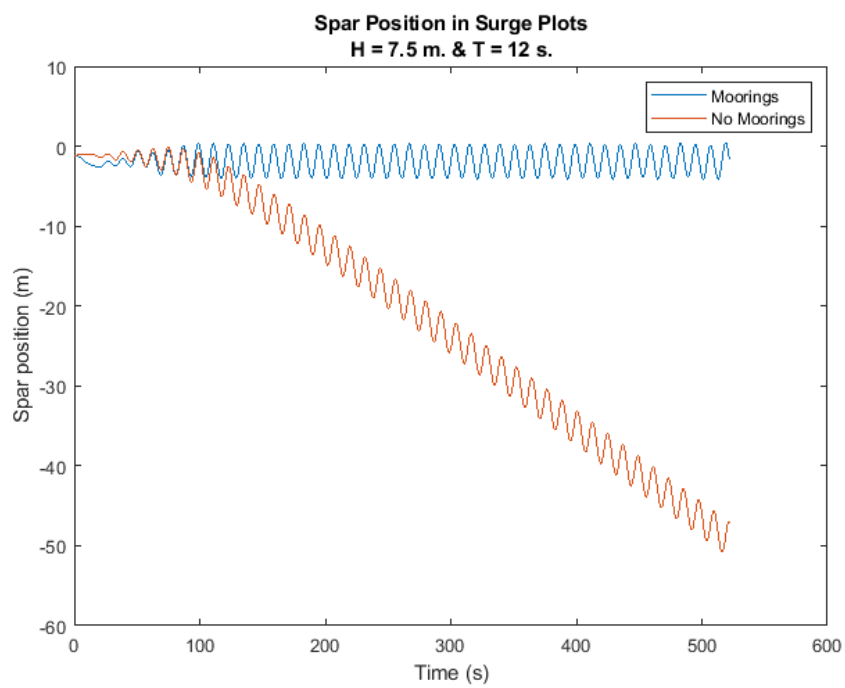

Figure 10: Spar Position in Surge Plots: H = 7.5 m. & T = 12 s.

Preliminary work consisted of comparing various WEC-Sim and ProteusDS results, such as forces and PTO velocity, to ensure the results obtained from ProteusDS would be representative

of the WEC-Sim case. A midwater float mooring system was attached to LUPA20, as shown in Figure 11, to conduct mooring analyses.

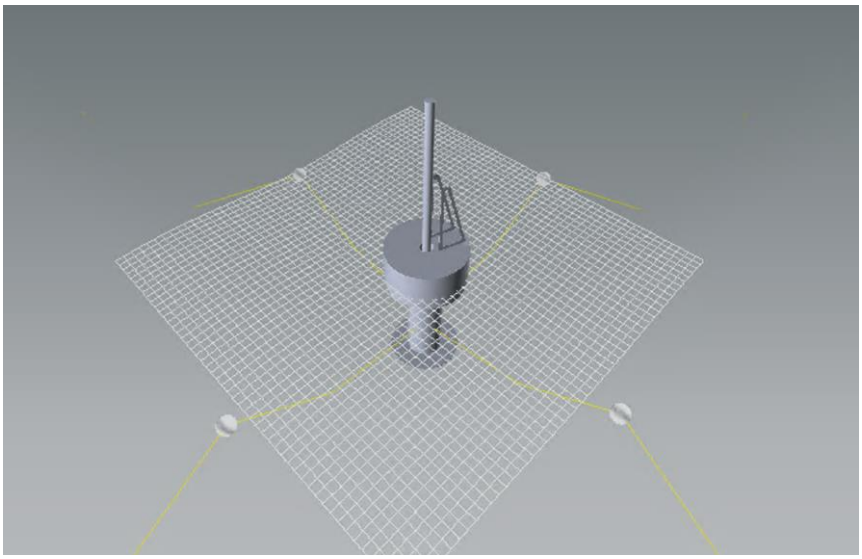

Figure 11: LUPA20 with a midwater float mooring setup in ProteusDS

ProteusDS Mooring Analysis

After the ProteusDS setup was complete, simulations using regular waves with extreme wave conditions were run to understand the effects that the mooring lines might have on the dynamics and power production of LUPA20. The extreme wave conditions were chosen based on sea states in the PacWave Wave Resource Assessment written by Dunkle et al. [31] and are shown in Table 1.

Table 1: Extreme Wave Conditions Used in the Mooring Analysis

Wave Height (m)	Wave Period (s)
5.0	8.0
6.0	9.0
7.0	10
7.5	11
7.5	12

To further analyze the effects of mooring lines on various parameters associated with LUPA20, a sensitivity study was conducted using the "optimal" PTO damping coefficients found in the WEC-Sim exhaustive PTO damping coefficient search as median values. The midwater float mooring setup was used and simulations were run for about 405 seconds in regular waves with the same wave periods used in the WEC-Sim PTO damping coefficient analysis. Five PTO damping coefficients were analyzed at each wave period to determine if the mooring line setup led the "optimal" PTO damping coefficient to deviate from the value determined in the WEC-Sim analysis.

WEC-Sim Transmission Coefficient Analysis

Conducting performance analyses and studying the effects of mooring lines provided many details regarding LUPA20. The transmission coefficient (K_t) is another parameter that is important to study because it provides insight into how much incident power from the waves is being converted to usable power by the WEC. In this study, the K_t was calculated based on the power available in the incoming wave and the average absorbed power due to the PTO. The wave conditions and "optimal" PTO damping coefficients used in the MAEP analysis were also used in the K_t analysis. Eq. 5 shows the equation for calculating the K_t. Eq. 6 is the PTO power equation that incorporates the "optimal" PTO damping coefficient for a certain wave period and the relative velocity between the float and the spar, and Eq. 7 is the incident wave power equation, which is calculated using the density of the fluid (ρ), gravitational acceleration (g), significant wave height (H_s), peak period (T_p), and the characteristic length of the float (D_{float}).

$$K_t = \sqrt{1 - \left(\frac{P_{PTO}}{P_{inc}}\right)} \tag{5}$$

$$P_{PTO} = C_{PTO} * v_{PTO,rel}^2 \tag{6}$$

$$P_{inc} = \frac{\rho * g^2}{64 * \pi} * H_s^2 * T_p * D_{float} \tag{7}$$

Results

The following section detail the results of this research. The subsections include PTO optimization, power performance assessment, numerical model comparison, mooring system impacts, and transmission coefficient analysis.

PTO Optimization

The preliminary step in analyzing the mean annual energy production of LUPA20 was to conduct an exhaustive damping coefficient search. This consisted of varying the wave period from 5 to 12 seconds and the PTO damping coefficient from 4E5 to 5E6 N*s/m. A constant wave height of 2 meters was chosen for this analysis. It was assumed for this analysis that wave height does not significantly affect the "optimal" PTO damping coefficient. Figure 12 details the results from the exhaustive PTO damping coefficient search. The average power is plotted using the "optimal" PTO damping coefficient determined for each sea state. The plot peaks at a power value of about 325 kW at about 9 seconds. This indicates that LUPA20's resonance period is about 9 seconds.

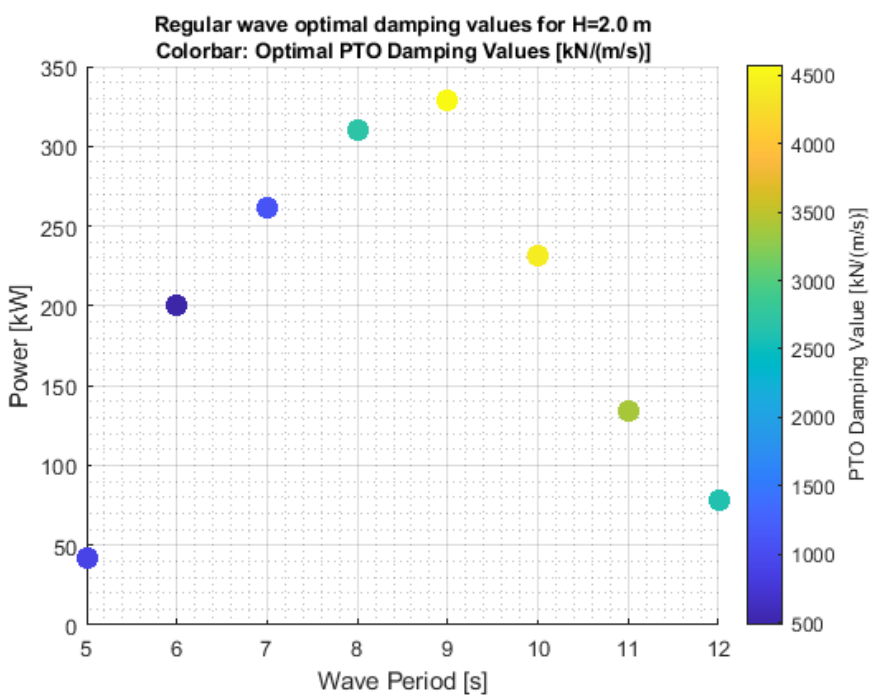

Figure 12: Exhaustive PTO Damping Coefficient Search Plot

Power Performance Assessment

The "optimal" PTO damping coefficients for each wave period were then used in the analysis of the mean annual energy production for LUPA20. Each bin in the bivariate histogram shown in Figure 13 shows the annual energy production for a particular sea state. The peak wave periods range from 5 to 12 seconds and the significant wave heights range from 0.5 to 7.5 m, which are based on sea states at PacWave. The annual energy production for each bin was determined by running each WEC-Sim case for about one hour of simulation time with a PM spectrum and multiplying the average power for each sea state by the hourly occurrence per year of the particular sea state based on sea states in the PacWave Wave Resource Assessment written by Dunkle et al. [31]. After summing the energy production from each bin, the total annual energy production was determined to be about 8.4E5 kWh. Based on this value, it was determined that LUPA20 has about an approximate power rating of 96 kW.

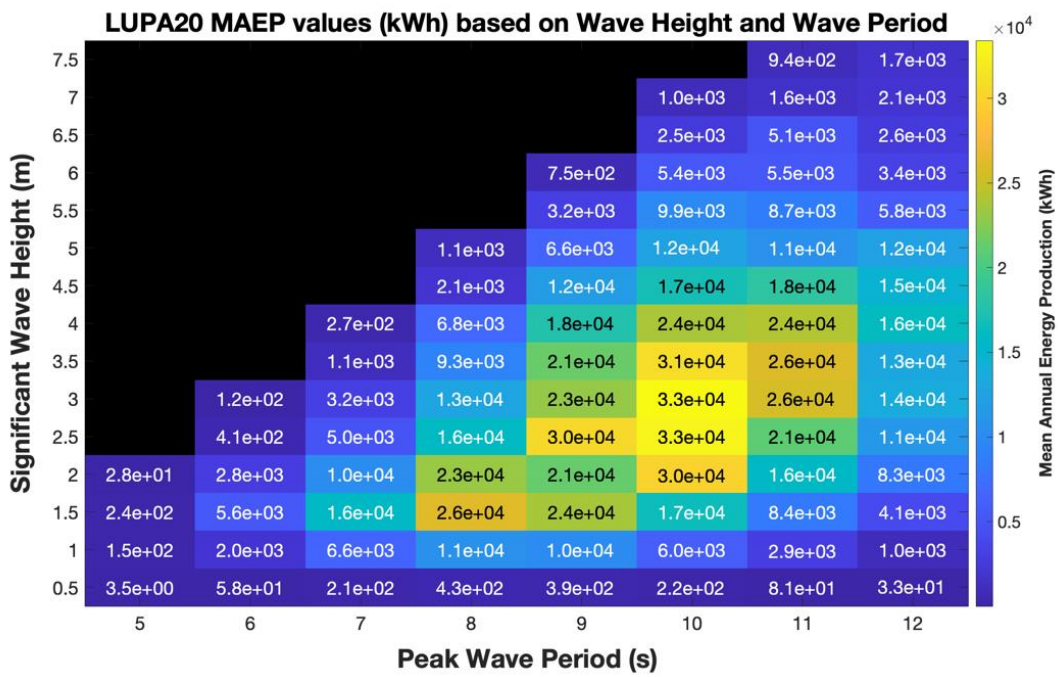

Figure 13: Mean Annual Energy Production Bivariate Histogram for LUPA20

Numerical Model Comparison

Due to importance of analyzing a comprehensive mooring design for LUPA20, a ProteusDS LUPA20 setup was developed. Excitation force, the relative velocity between the float

and the spar (PTO velocity), and PTO force were first compared between the WEC-Sim and ProteusDS models to help ensure the dynamics were similar. Figures 14 and 15 detail a portion of the time domain excitation force results for the float and the spar, respectively. The percent difference between the WEC-Sim and ProteusDS plots in Figures 14 and 15 are about 0.45% and 5.7%, respectively, which helps demonstrate the similarity between the WEC-Sim and ProteusDS setups. Figures 16 and 17 detail a portion of the time domain PTO velocity and PTO force results, respectively. The percent difference between the WEC-Sim and ProteusDS plots in Figures 16 and 17 are about 3.1% and 1.3%, respectively. The effects of the phase shift, which is evident in Figure 14 through 17, were assumed to be negligible due to the overall dynamics of the system having a greater effect on the parameters analyzed in this research.

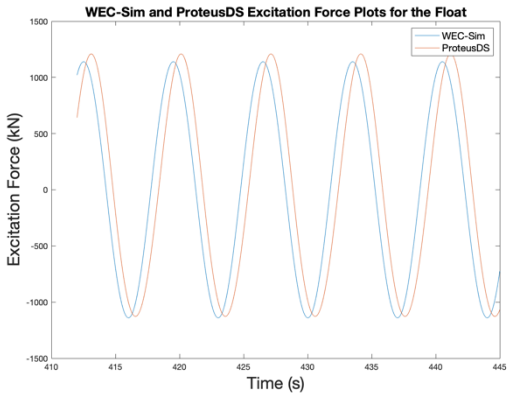

Figure 14: WEC-Sim and ProteusDS Float Excitation Force Comparison

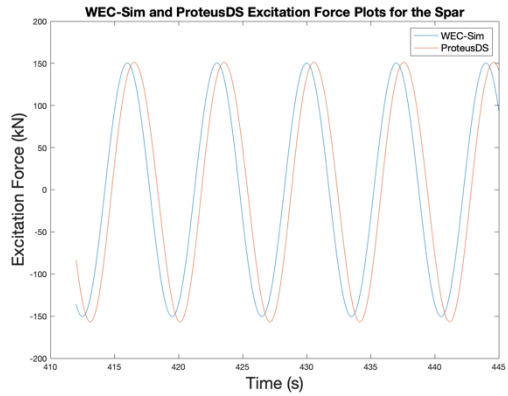

Figure 15: WEC-Sim and ProteusDS Spar Excitation Force Comparison

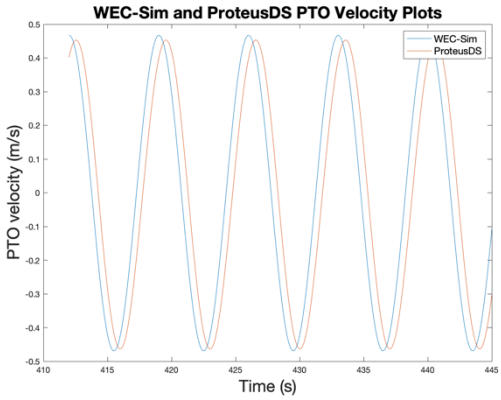

Figure 16: WEC-Sim and ProteusDS PTO Velocity Comparison

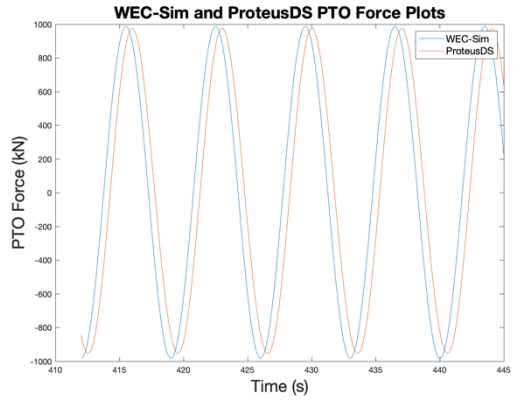

Figure 17: WEC-Sim and ProteusDS PTO Force Comparison

Mooring System Impacts

After developing the ProteusDS LUPA20 setup, simulations were run with a range of extreme sea states for a moored and not moored setup. Each simulation was run for 522 seconds and used regular waves. The approximate peak PTO power, average PTO power, and peak-to-average ratios values for the simulation that led to the largest percent difference between the peak-to-average PTO power values between the mooring and no mooring cases are shown in Table 2. The percent difference between the peak to average PTO power values between the mooring and no mooring cases is about 4.9%. The percent difference between the average PTO power values between the mooring and no mooring cases is about -6.4%. The percent difference between the

peak-to-average PTO power values between the mooring and no mooring cases is about 12%. Figure 18 shows the time-domain simulation power results from the simulation consisting of a 7.5 meter wave height and a 12 second wave period. Based on the PTO power results shown in Figure 18, the mooring setup has a relatively significant impact on the power absorbed by the PTO. The plots for the other extreme wave sea states are provided in the appendix. Those plots also indicate that the mooring system has a relatively significant impact on power performance.

Table 2: PTO power statistics for the H = 7.5 m. & T = 12 s. mooring analysis simulation case

H = 7.5 m. T = 12 s.	Peak PTO Power (kW)	Average PTO Power (kW)	Peak-to-average PTO Power
Mooring	2584	841.1	3.072
No Mooring	2463	898.8	2.741

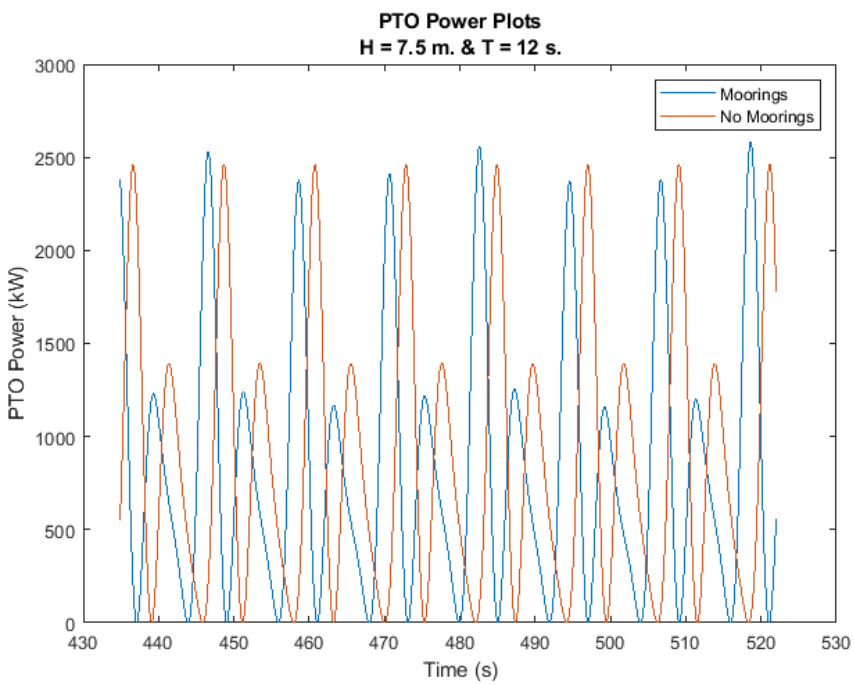

Figure 18: PTO Power Plots: H = 7.5 m. & T = 12 s.

To continue investigating the effects mooring lines have on the performance of LUPA20, a PTO damping coefficient sensitivity study was conducted between the WEC-Sim setup and the

ProteusDS setup with mooring lines. ProteusDS simulations were run with a variety PTO damping coefficients that were based on the "optimal" ones determined in the WEC-Sim analysis. Figure 19 shows the amount of power produced for a range of sea states with the associated "optimal" PTO damping coefficient for the ProteusDS setup with mooring lines. When compared to the WEC-Sim results in Figure 20, the "optimal" PTO damping coefficients are all the same. However, when analyzing the power values shown in Figures 19 and 20, besides the case with a wave period of 5 seconds, the WEC-Sim average power values are greater than the ProteusDS average power values. The largest percent difference between the average power values is approximately 16% and occurs for the case with a wave period of 12 seconds.

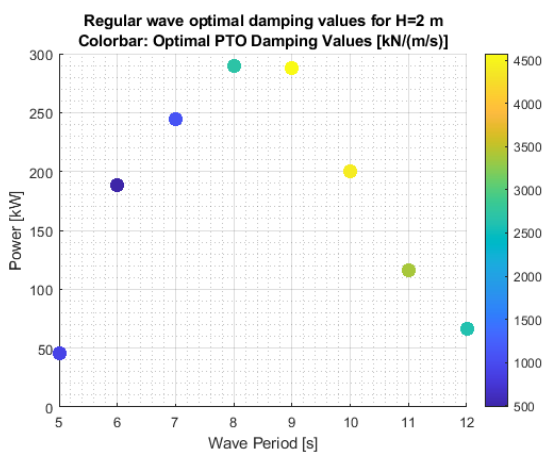

Figure 19: ProteusDS setup with mooring lines: PTO Damping Coefficient Comparison Results

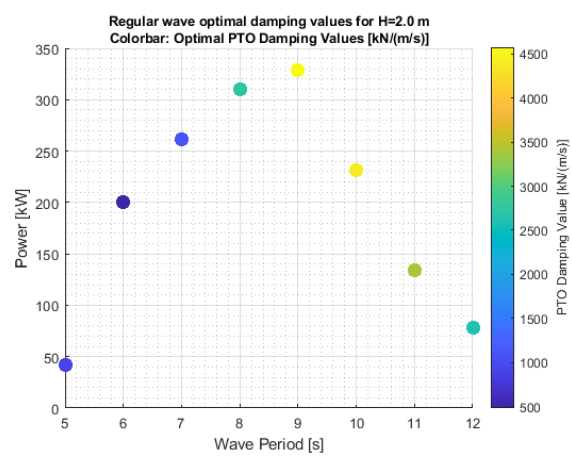

Figure 20: WEC-Sim setup without mooring lines: Exhaustive PTO Damping Coefficient Search Results

Transmission Coefficient Analysis

Another performance metric analyzed was the effect LUPA20 has on the incoming waves. This process involved analyzing how much energy LUPA20 extracts from the incoming waves and the impact LUPA20 has on downstream wave conditions. The K_t analysis described in the methods section was used and Eq. 5 was used to calculate the amount of power LUPA20 absorbed compared to the power in the incoming wave. The WEC-Sim setup, simulation parameters, and sea states remained the same between this analysis and the MAEP analysis. After calculating the K_t for each sea state, Figure 21 was developed. The smallest K_t, which indicates the highest

percentage of absorbed power from the incoming wave, is 0.84. A K_t of 0.84 occurs for 8 and 9 second wave periods. The peak wave period with the largest average power value from the WEC-Sim exhaustive PTO damping coefficient search is 9 seconds. Figure 21 also indicates a lack of dependence of significant wave height on the K_t. The K_t varies by less than about 4% over each range of significant wave heights for each peak wave period.

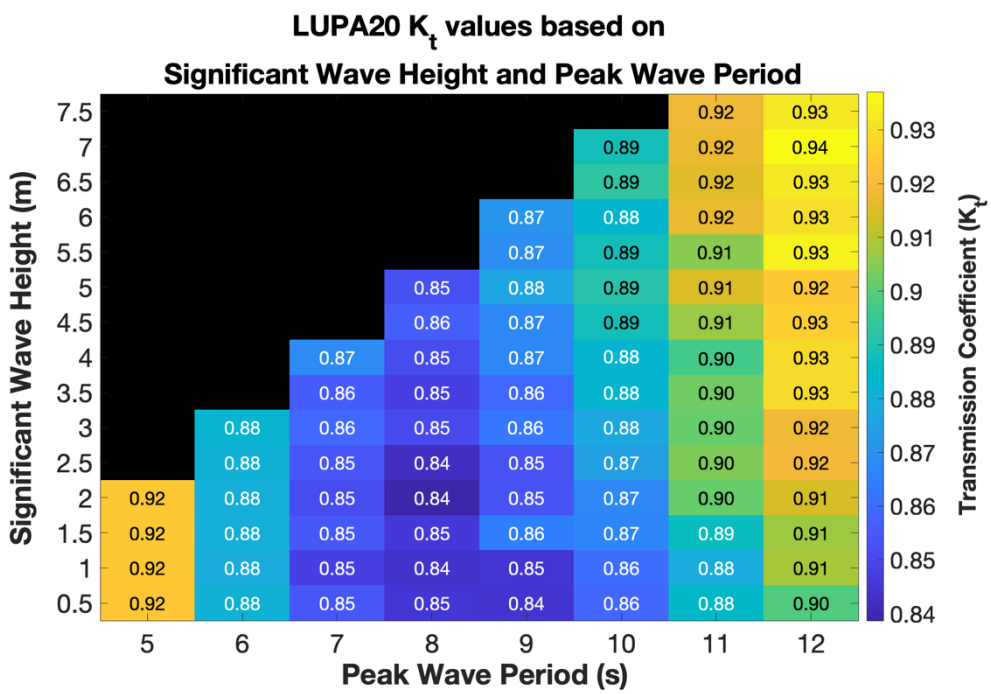

Figure 21: Transmission Coefficient (K_t) Bivariate Histogram for LUPA20

Discussion

There is continuing to be a need for reliable and efficient renewable energy technologies. This need has led WEC developers and researchers to continue improving and analyzing WEC archetypes to maximize the capabilities of the devices. The previous sections provided details regarding power capabilities and effects mooring lines have on a full-scale WEC.

PTO Optimization and Power Performance Assessment

The analysis of the effects of the PTO damping coefficient on power production and the energy production capabilities of LUPA20 provided information regarding the potential for full-scale point absorbers to provide significant energy to communities. As discussed, the resonance

period of LUPA20 was determined to be about 9 seconds, which is reasonable for the size of this device. Furthermore, understanding which wave period leads to the most power production helps WEC developers know what locations will be the most optimal for LUPA20. As discussed in the PacWave Wave Resource Assessment written by Dunkle et al. [31], the most commonly occurring energy period at PacWave is 8.5 seconds. This indicates PacWave has the potential to be an optimal location for LUPA20 based on LUPA20's resonance period being 9 seconds.

Mooring System Impacts

Results from the mooring analyses provided many details regarding the impacts mooring lines have on the performance of LUPA20. The findings from each extreme wave state simulation indicated that the mooring lines have a significant impact on the peak and mean PTO power absorbed from the incoming waves. This is indicated by the percent difference between the mooring and no mooring cases being approximately 4.7% for peak PTO power and approximately 6.9% for average PTO power. The effects mooring lines have on peak-to-average PTO power were also analyzed because the peak-to-average PTO power is essential for understanding the variability in power production. Results indicate that the peak-to-average PTO power for the mooring cases is approximately 13% larger than the no mooring case. The significantly larger peak-to-average ratio for the mooring case indicates the importance of considering the effects mooring lines can have on power production variability.

The findings from the PTO damping coefficient sensitivity analysis indicated a lack of dependency between PTO damping coefficients and mooring lines. Those results lead to the conclusion that mooring lines do not have a significant impact on "optimal" PTO damping coefficients. However, the results showed the average power decreased over most of the wave periods for the ProteusDS with mooring case when compared to the WEC-Sim case. Overall, these findings provide preliminary results that could be expanded upon in future work. It will be essential to run more simulations to better understand the impacts of mooring lines. To reduce computational time in the PTO damping coefficient sensitivity analysis, a small range of PTO damping coefficients and sea states was used. The results may vary if a more refined range of PTO damping coefficients and a wider range of sea states were incorporated into future work.

Transmission Coefficient Analysis

The K_t analysis provided insight regarding the performance of LUPA20. The smallest K_t of 0.84 helps provide evidence that LUPA20 does considerably affect the incoming waves, even when only considering the incident power and PTO power in the K_t calculation. Another important finding from the K_t analysis is the K_t values do not have a strong dependence on the wave height. This result could indicate a linear relationship between the incident power and the absorbed power. For example, as the wave height increases, the relative velocity of the spar and the float could increase by a similar factor, which, when Eq. 5 is applied, would not significantly change the K_t. The trend could also arise from using a mainly linear model to represent LUPA20, instead of a nonlinear model. Furthermore, the K_t analysis results could suggest a correlation between the "optimal" PTO damping coefficient and the wave height. This study limited the exhaustive PTO damping coefficient search to not varying the wave height, however future research could be conducted into the effects wave height has on "optimal" PTO damping coefficients.

Conclusion

The use of more renewable energy technologies is critical to a sustainable future. WECs can be an integral component of the sustainable development of communities, which is why researching the performance of a variety of WECs is critical to meeting sustainability goals. This study analyzed the performance of a particular WEC called LUPA20, which is a twenty-times scaled version of a WEC being developed at Oregon State University. The research consisted of four main objectives. The first objective was determining the performance of LUPA20 in a variety of sea states and with a variety of PTO damping coefficients. Following the development and analysis of LUPA20 in WEC-Sim, it was of great interest to study the effects mooring lines might have on the performance of LUPA20. The mooring analyses were conducted by analyzing the impacts mooring lines have on power production and "optimal" PTO damping coefficients. A K_t analysis was also conducted to understand how LUPA20 is affecting the incoming waves.

PTO Optimization and Power Performance Assessment

To achieve the first objective, an exhaustive PTO damping coefficient search and MAEP analysis were conducted. It was determined that LUPA20's resonance period is about 9 seconds, which is similar to the most commonly occurring energy period at PacWave being 8.5 seconds

[31]. Furthermore, the MAEP was determined to be about 8.4E5 kWh, which means LUPA20 has an approximate power rating of 96 kW. As this study used wave conditions based on one specific location, future work could consist of analyzing the performance of LUPA20 in other locations.

Mooring System Impacts

Objectives two and three were primally focused on the effects of mooring lines. The results indicated the percent difference of the peak powers and average powers when comparing the mooring and no mooring cases are about 4.7% and 6.9%, respectively. Furthermore, the peak-to-average ratio for the mooring case is about 13% larger than the no mooring case. The PTO damping coefficient sensitivity analysis indicated a lack of strong dependency between the mooring system and "optimal" PTO damping coefficients. However, the ProteusDS mooring case did have reduced average powers for most of the wave periods, with the maximum percent difference being about 16%. Future work should consist of using a more refined range of PTO damping values and sea states to further analyze the effects of using mooring lines. Furthermore, this study only considered the effects that mooring lines have on LUPA20's PTO power, which provides an opportunity for future work to consist of analyzing the effects mooring lines have on other means of absorbing power from the incoming waves.

Transmission Coefficient Analysis

The impacts that LUPA20 has on the incoming waves were studied by conducting a K_t analysis over a range of sea states at PacWave. The smallest K_t was determined to be 0.84, which means about 16% of the incoming wave power was absorbed by LUPA20. The K_t analysis methodology discussed in the methods section could be used to study the effects arrays of LUPA20s have on the ocean environment. Such arrays have the potential to reduce peak-to-average PTO power. Findings also showed that the wave height did not have a significant impact on the K_t. One explanation for this finding is that the "optimal" PTO damping coefficient does depend on wave height. It will be important in future work to study the effects that wave heights have on "optimal" PTO damping coefficients and K_t values.

Findings from the analysis of LUPA20 provided insights into the performance of LUPA20, the impacts of mooring lines, and the effect LUPA20 has on the ocean environment. The MAEP analysis provided information regarding the power production capabilities of LUPA20. Results from the mooring analysis provided insights into the effects mooring lines have on the performance

of LUPA20 and provided a framework for future research to be conducted. Furthermore, the K_t analysis provided information regarding LUPA20's impact on incoming waves. The overall methodology used to conduct this research could provide WEC developers with a framework to analyze and develop more efficient WECs to help provide renewable energy technologies to more communities.

References

[1] "Wave power - U.S. Energy Information Administration (EIA)." https://www.eia.gov/energyexplained/hydropower/wave-power.php (accessed Oct. 16, 2021).

[2] K. BUDAR and J. FALNES, "A resonant point absorber of ocean-wave power," *Nat. 1975 2565517*, vol. 256, no. 5517, pp. 478–479, Aug. 1975, doi: 10.1038/256478a0.

[3] Y. Zhang, B. Teng, and Y. Gou, "Nonlinear modelling of a point-absorber wave energy converter based on the weak-scatterer approximation," *Ocean Eng.*, vol. 239, p. 109924, Nov. 2021, doi: 10.1016/J.OCEANENG.2021.109924.

[4] "PB3 PowerBuoy® - Ocean Power Technologies." https://oceanpowertechnologies.com/pb3-powerbuoy/ (accessed Nov. 19, 2021).

[5] "Technology." https://www.corpowerocean.com/technology/#corpowerConcept (accessed Nov. 19, 2021).

[6] E. Arzaghi, M. M. Abaei, R. Abbassi, M. O'Reilly, V. Garaniya, and I. Penesis, "A Markovian approach to power generation capacity assessment of floating wave energy converters," *Renew. Energy*, vol. 146, pp. 2736–2743, Feb. 2020, doi: 10.1016/J.RENENE.2019.08.099.

[7] X. Zhao and D. Ning, "Experimental investigation of breakwater-type WEC composed of both stationary and floating pontoons," *Energy*, vol. 155, pp. 226–233, Jul. 2018, doi: 10.1016/J.ENERGY.2018.04.189.

[8] V. Piscopo and A. Scamardella, "Design of a new point absorber with a fully submerged toroidal shape," *Ocean Eng.*, vol. 191, p. 106492, Nov. 2019, doi: 10.1016/J.OCEANENG.2019.106492.

[9] M. Shadman, S. F. Estefen, C. A. Rodriguez, and I. C. M. Nogueira, "A geometrical optimization method applied to a heaving point absorber wave energy converter," *Renew. Energy*, vol. 115, pp. 533–546, Jan. 2018, doi: 10.1016/J.RENENE.2017.08.055.

[10] V. Piscopo, G. Benassai, L. Cozzolino, R. Della Morte, and A. Scamardella, "A new optimization procedure of heaving point absorber hydrodynamic performances," *Ocean Eng.*, vol. 116, pp. 242–259, Apr. 2016, doi: 10.1016/J.OCEANENG.2016.03.004.

[11] İ. Ö. Erselcan and A. Kükner, "A parametric optimization study towards the preliminary design of point absorber type wave energy converters suitable for the Turkish coasts of the

Black Sea," *Ocean Eng.*, vol. 218, p. 108275, Dec. 2020, doi: 10.1016/J.OCEANENG.2020.108275.

[12] X. Li, C. Liang, C. A. Chen, Q. Xiong, R. G. Parker, and L. Zuo, "Optimum power analysis of a self-reactive wave energy point absorber with mechanically-driven power take-offs," *Energy*, vol. 195, p. 116927, Mar. 2020, doi: 10.1016/J.ENERGY.2020.116927.

[13] S. J. Beatty, M. Hall, B. J. Buckham, P. Wild, and B. Bocking, "Experimental and numerical comparisons of self-reacting point absorber wave energy converters in regular waves," *Ocean Eng.*, vol. 104, pp. 370–386, Aug. 2015, doi: 10.1016/J.OCEANENG.2015.05.027.

[14] X. Dong, Z. Gao, D. Li, and H. Shi, "Experimental and numerical study of a two-body heaving wave energy converter with different power take-off models," *Ocean Eng.*, vol. 220, p. 108454, Jan. 2021, doi: 10.1016/J.OCEANENG.2020.108454.

[15] M. T. Rahmati and G. A. Aggidis, "Numerical and experimental analysis of the power output of a point absorber wave energy converter in irregular waves," *Ocean Eng.*, vol. 111, pp. 483–492, Jan. 2016, doi: 10.1016/J.OCEANENG.2015.11.011.

[16] "Wamit, Inc. - The State of the Art in Wave Interaction Analysis." https://www.wamit.com/ (accessed Feb. 03, 2021).

[17] Y. Ma, A. Zhang, L. Yang, H. Li, Z. Zhai, and H. Zhou, "Motion simulation and performance analysis of two-body floating point absorber wave energy converter," *Renew. Energy*, vol. 157, pp. 353–367, Sep. 2020, doi: 10.1016/J.RENENE.2020.05.026.

[18] E. J. Ransley, D. M. Greaves, A. Raby, D. Simmonds, M. M. Jakobsen, and M. Kramer, "RANS-VOF modelling of the Wavestar point absorber," *Renew. Energy*, vol. 109, pp. 49–65, Aug. 2017, doi: 10.1016/J.RENENE.2017.02.079.

[19] J. P. Ortiz, "The Influence of Mooring Dynamics on the Performance of Self Reacting Point Absorbers," 2006.

[20] F. Cerveira, N. Fonseca, and R. Pascoal, "Mooring system influence on the efficiency of wave energy converters," *Int. J. Mar. Energy*, vol. 3–4, pp. 65–81, Dec. 2013, doi: 10.1016/J.IJOME.2013.11.006.

[21] B. Zanuttigh, E. Angelelli, and J. P. Kofoed, "Effects of mooring systems on the performance of a wave activated body energy converter," *Renew. Energy*, vol. 57, pp.

422–431, Sep. 2013, doi: 10.1016/J.RENENE.2013.02.006.

[22] S. Xu, S. Wang, and C. Guedes Soares, “Experimental investigation on the influence of hybrid mooring system configuration and mooring material on the hydrodynamic performance of a point absorber,” *Ocean Eng.*, vol. 233, p. 109178, Aug. 2021, doi: 10.1016/J.OCEANENG.2021.109178.

[23] P. C. Vicente, A. F. O. Falcão, and P. A. P. Justino, “Nonlinear dynamics of a tightly moored point-absorber wave energy converter,” *Ocean Eng.*, vol. 59, pp. 20–36, Feb. 2013, doi: 10.1016/J.OCEANENG.2012.12.008.

[24] N. Zhang, X. Zhang, L. Xiao, H. Wei, and W. Chen, “Evaluation of long-term power capture performance of a bistable point absorber wave energy converter in South China Sea,” *Ocean Eng.*, vol. 237, p. 109338, Oct. 2021, doi: 10.1016/J.OCEANENG.2021.109338.

[25] S. Heo and W. Koo, “Numerical procedures for dynamic response and reaction force analysis of a heaving-point absorber wave energy converter,” *Ocean Eng.*, vol. 200, p. 107070, Mar. 2020, doi: 10.1016/J.OCEANENG.2020.107070.

[26] “Rhino - Rhinoceros 3D.” https://www.rhino3d.com/ (accessed Oct. 25, 2021).

[27] “Boundary Element Method Input/Output (bemio) Documentation and Users Guide — bemio v1.0a0 documentation.” https://wec-sim.github.io/bemio/ (accessed Oct. 25, 2021).

[28] “WEC-Sim (Wave Energy Converter SIMulator) — WEC-Sim documentation.” https://wec-sim.github.io/WEC-Sim/master/index.html (accessed Oct. 25, 2021).

[29] by Scott James Beatty BASc, “Self-Reacting Point Absorber Wave Energy Converters,” 2015, Accessed: Nov. 12, 2021. [Online]. Available: https://dspace.library.uvic.ca/handle/1828/6620.

[30] H. Gu, P. Stansby, T. Stallard, and E. Carpintero Moreno, “Drag, added mass and radiation damping of oscillating vertical cylindrical bodies in heave and surge in still water,” *J. Fluids Struct.*, vol. 82, pp. 343–356, Oct. 2018, doi: 10.1016/J.JFLUIDSTRUCTS.2018.06.012.

[31] G. Dunkle, B. Robertson, G. Garcia-Medina, and Z. Yang, “PacWave Wave Resource Assessment.” 2020, Accessed: Oct. 25, 2021. [Online]. Available: https://ir.library.oregonstate.edu/concern/technical_reports/hm50tz68v?locale=en.

[32] “Statistical description of wave parameters - Coastal Wiki.”

http://www.coastalwiki.org/wiki/Statistical_description_of_wave_parameters (accessed Nov. 12, 2021).

[33] “ProteusDS | A flexible Dynamic Analysis Tool for Ocean Industries | DSA.” https://dsaocean.com/proteusds/overview/ (accessed Oct. 25, 2021).

[34] “The Drag Equation.” https://www.grc.nasa.gov/www/k-12/airplane/drageq.html (accessed Nov. 12, 2021).

[35] “Advanced Features — WEC-Sim documentation.” https://wec-sim.github.io/WEC-Sim/dev/user/advanced_features.html (accessed Nov. 12, 2021).

[36] “Overview — WEC-Sim documentation.” https://wec-sim.github.io/WEC-Sim/master/theory/theory.html?highlight=mooring#mooring (accessed Nov. 04, 2021).

[37] PacWave, "TESTING WAVE ENERGY FOR THE FUTURE," 31 March 2022. [Online]. Available: https://pacwaveenergy.org/.

Appendix

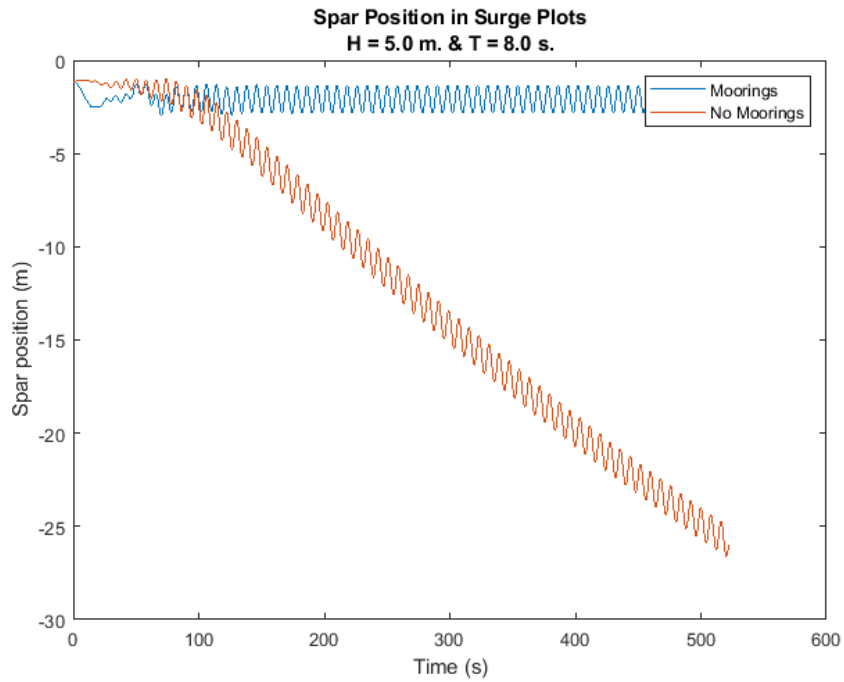

Figure 22: Spar Position in Surge Plots: H = 5.0 m. & T = 8.0 s.

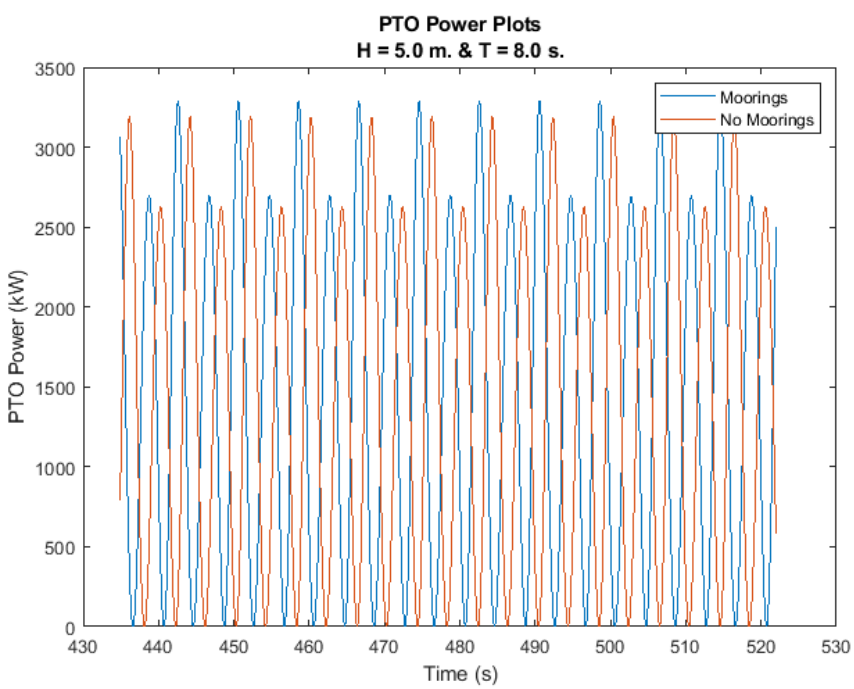

Figure 23: PTO Power Plots: H = 5.0 m. & T = 8.0 s.

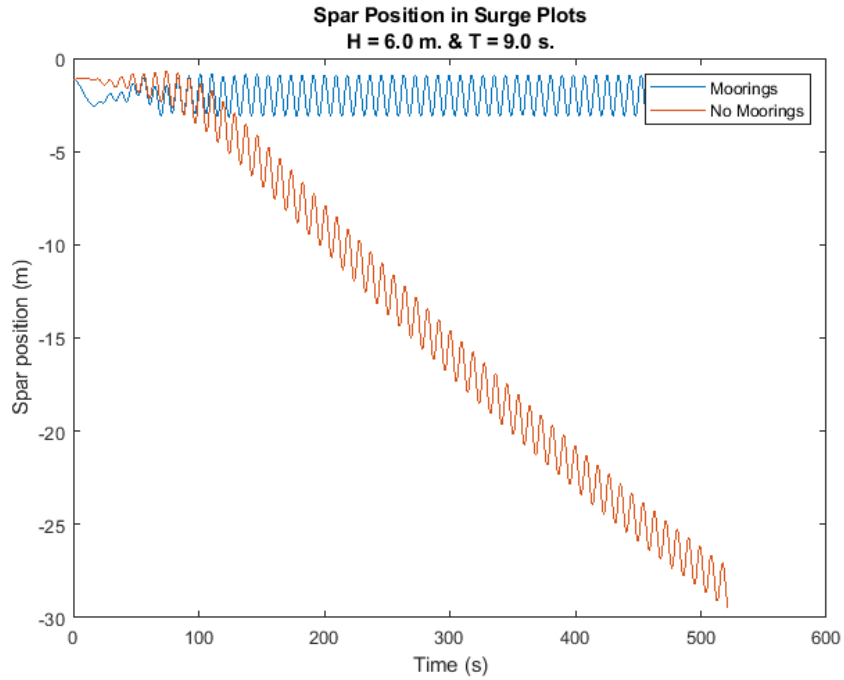

Figure 24: Spar Position in Surge Plots: H = 6.0 m. & T = 9.0 s.

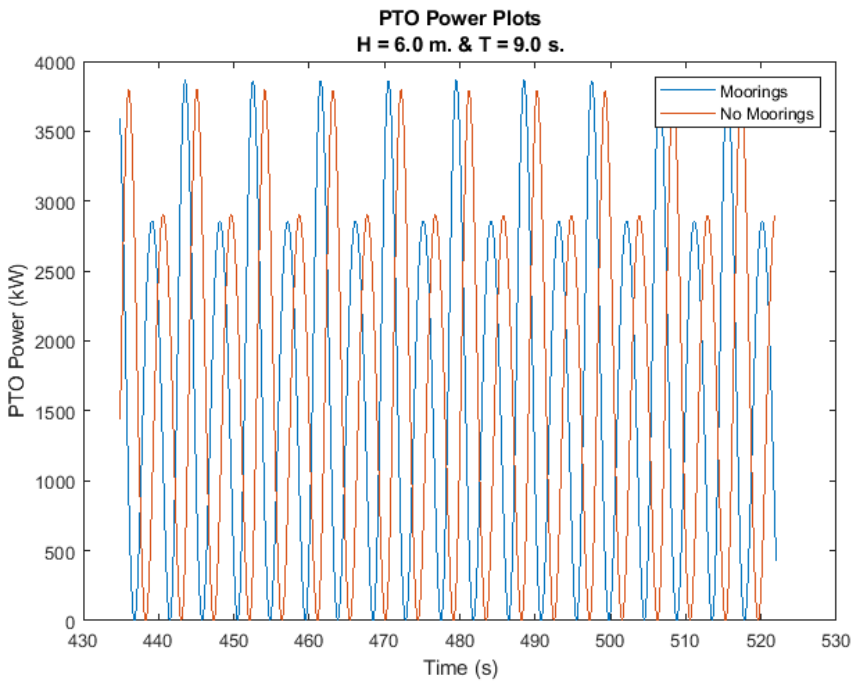

Figure 25: PTO Power Plots: H = 6.0 m. & T = 9.0 s.

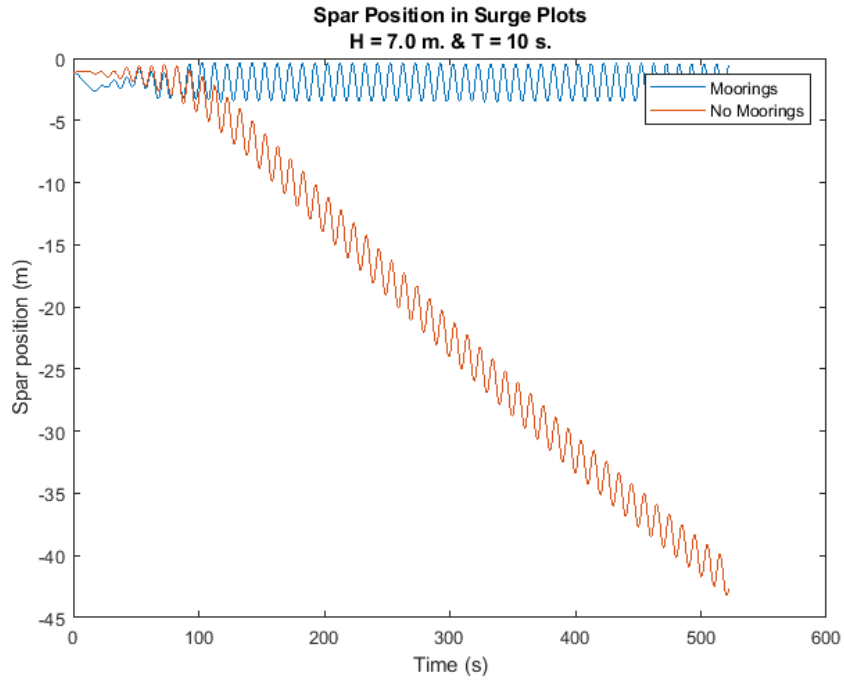

Figure 26: Spar Position in Surge Plots: H = 7.0 m. & T = 10 s.

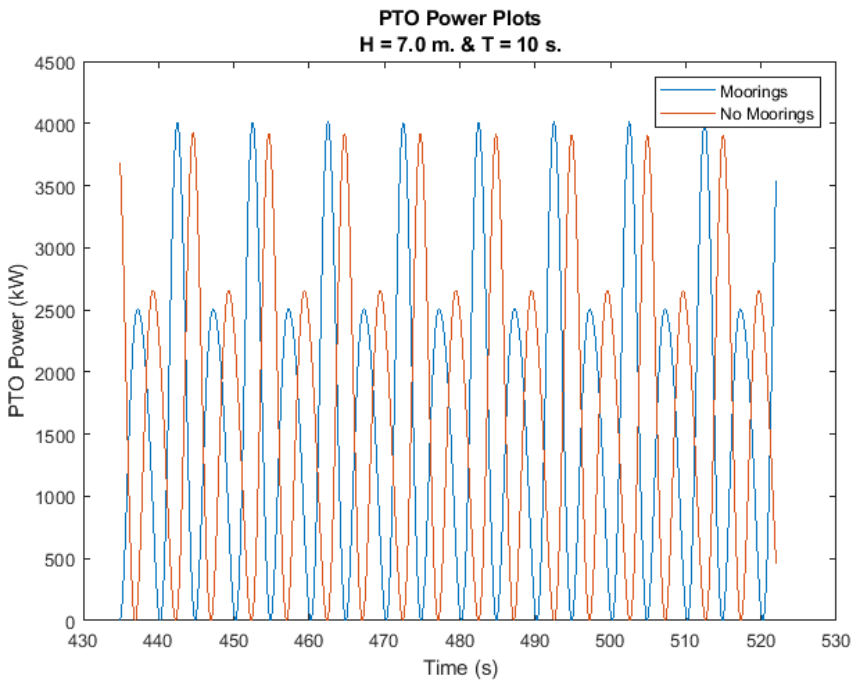

Figure 27: PTO Power Plots: H = 7.0 m. & T = 10 s.

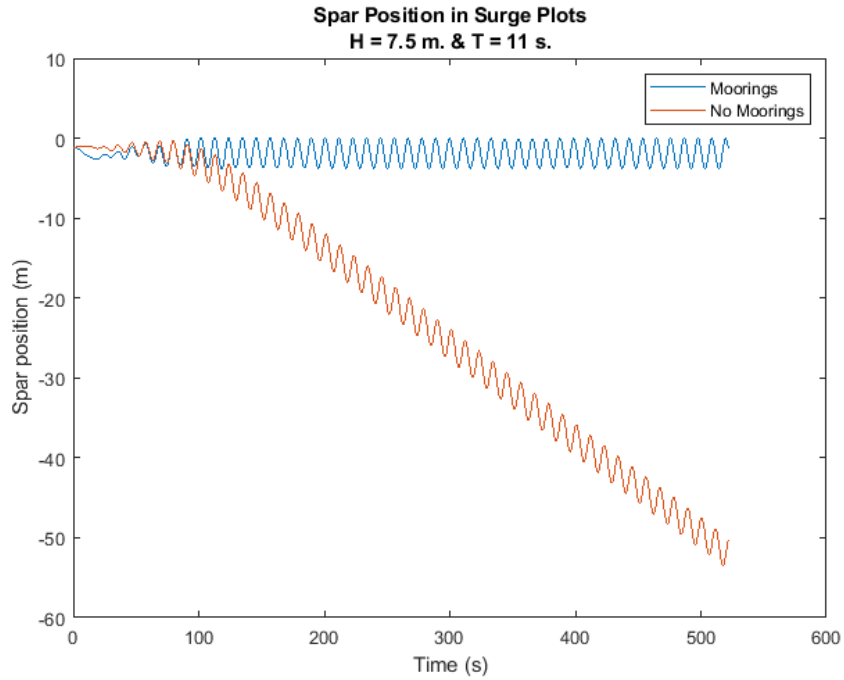

Figure 28: Spar Position in Surge Plots: H = 7.5 m. & T = 11 s.

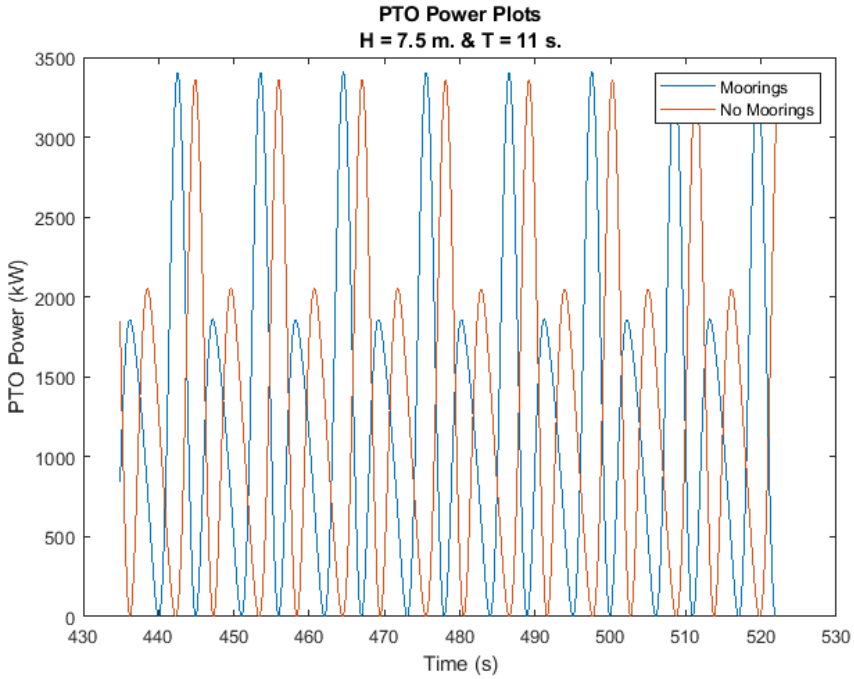

Figure 29: PTO Power Plots: H = 7.5 m. & T = 11 s.